A Cross-Layer Diversity Technique for Multicarrier OFDM Multimedia Networks

Yee Sin Chan, *Member, IEEE*, Pamela C. Cosman, *Senior Member, IEEE*, and Laurence B. Milstein, *Fellow, IEEE*

***Abstract*—Diversity can be used to combat multipath fading and improve the performance of wireless multimedia communication systems. In this work, by considering transmission of an embedded bitstream over an orthogonal frequency division multiplexing (OFDM) system in a slowly varying Rayleigh faded environment, we develop a cross-layer diversity technique which takes advantage of both multiple description coding and frequency diversity techniques. More specifically, assuming a frequency-selective channel, we study the packet loss behavior of an OFDM system and construct multiple independent descriptions using an FEC-based strategy. We provide some analysis of this cross-layer approach and demonstrate its superior performance using the set partitioning in hierarchical trees image coder.**

***Index Terms*—Cross-layer design, diversity, frequency diversity, multimedia communications, multiple description coding, orthogonal frequency division multiplexing (OFDM), progressive transmission, wireless video.**

I. Introduction

DIVERSITY is an important means to improve the performance of mobile wireless systems over fading channels. The opportunity for diversity gain of a communication system arises whenever there are multiple channels over which the fading is not highly correlated. The opportunity can be exploited by channel coding across these parallel fading components at the physical layer. Commonly used physical layer techniques include temporal, spatial, and frequency diversity. In temporal diversity, channel coding plus interleaving is used in the time domain to transmit the signal. For the technique to be effective, the time frame has to be greater than the coherence time (time-selective channel). Frequency diversity can be achieved by adding redundancy across multiple RF carriers in a frequency-selective channel. In spatial diversity, multiple antennas with spacing greater than the coherence distance are used to transmit and receive multiple replicas of the signal.

Since physical layer diversity gain is achieved by introducing redundancy across the independent parallel components, if all the parallel components are used for transmitting independent information bits, the opportunity for diversity gain is not being exploited [1]. However, through source coding techniques, specifically, multiple description coding, it is possible for a source coder at the application layer to take advantage of the parallel independent components provided. Analogous to the physical layer diversity techniques offered by channel coding, this has sometimes been referred to as *application layer diversity* [2] or source-based diversity [3].

Earlier studies of multiple description source coding concentrated on the fundamental information-theoretic bounds for specific input source models [4]–[6]. Recently, largely driven by the explosive demand for multimedia services over both wired and wireless networks, practical implementation of multiple description source coding has received a lot of attention (see [7] for a review). A multiple description source coder generates multiple bitstreams (descriptions) of the source such that each description individually describes the source with a certain level of fidelity. The multiple bitstreams are transmitted over the network, and the correctly received descriptions are then individually decoded and synergistically combined to enhance the end-user received quality. Due to the individually decodable nature of the multiple descriptions, the loss of some of the descriptions will not jeopardize the decoding of correctly received descriptions, while the fidelity of the received information improves as the number of received descriptions increases.

In order to achieve the best performance, multiple description coding generally requires the existence of *multiple independent* channels. Consider a simple example regarding the transmission of two individually decodable descriptions. If both descriptions are transmitted in highly correlated channels, then in most of the cases, the two descriptions would either be both lost or both received. Hence, relatively little advantage can be achieved by using multiple description coding and making each description individually decodable. Despite the importance of this fundamental concept, the construction of multiple descriptions is usually considered as a pure source coding technique in which the existence of multiple independent channels, or equivalently the order of diversity, is either presumed [3], [8]–[10] or neglected [11], [12]. While the assumption of the existence of multiple independent channels is usually questionable, the lack of consideration of the order of diversity available may sometimes lead to unnecessarily tight constraints on the construction of multiple description coders. As stated previously, the construction of a multiple description coder usually involves having each description *individually* decodable such that when only one of the descriptions is available, a very low level of fidelity can still be achieved. However, if the number of independent channels is large, the probability of the simultaneous failure of all but one of them will be very small. Hence, the unnecessarily tight constraint that each description be individually decodable may

Manuscript received April 21, 2004; revised April 20, 2005. This work was supported in part by Ericsson, the Center for Wireless Communications at UCSD, the California Institute for Telecommunications and Information Technology (Calit2), and the UC Discovery Grant Program. The associate editor coordinating the review of this manuscript and approving it for publication was Dr. John Apostolopoulos.

The authors are with the Department of Electrical and Computer Engineering, University of California at San Diego, La Jolla, CA 92093-0407 USA (e-mail: chanys@ieee.org; pcosman@code.ucsd.edu; milstein@ece.ucsd.edu).

Digital Object Identifier 10.1109/TIP.2005.863967

eventually lead to inefficient overall system design. More importantly, the construction of multiple descriptions usually involves adding redundancy at the source coder. Typically, the composite quality using multiple description coding is less than that achievable with a single description at the same source coding rate [3], [10], [11].

In fact, the necessity for the consideration of the order of diversity for the transmission of multiple descriptions has gradually been realized by some researchers when studying the transmission of multiple descriptions over wired networks. Hence, multiple independent paths are created at the network layer through routing for the transmission of individually decodable descriptions. This method is generally referred to as path diversity [13], [14]. In wireless communications, the term "path diversity" traditionally means the reception of multiple replicas of the same signal due to the multiple resolvable paths in the wireless environment [15]. However, the term "path diversity" in [13], [14] refers to the transmission of the multiple descriptions over separate routing paths. The use of separate routing paths at the network layer was shown to be able to improve the effectiveness of multiple description coding over the wired networks due to more desirable packet loss characteristics [13], [14].

In wireless communication systems, unlike wired networks, multiple independent channels may sometimes exist at the physical layer due to the effect of multipath fading. Unfortunately, this is usually neglected in the transmission schemes employing multiple description coding. For example, the transmission of multiple descriptions is considered in a single-carrier mobile wireless system in [16] and in a MIMO-OFDM system in [17]. In particular, both works considered employing the FEC-based multiple description coding proposed in [11], [18], [19]. However, neither [16] nor [17] took into consideration the order of diversity at the physical layer and the use of physical layer diversity techniques.

On the other hand, while the importance of multiple independent components for employing physical diversity techniques is well-studied and understood in wireless communications, the employing of channel coding across multiple independently faded components generally requires a reduction in information rate. In other words, a higher diversity gain is typically achieved at the expense of a reduced information rate. Although the bit error rate of a wireless communication system is generally a strictly decreasing function of the order of diversity, the gain diminishes with increasing order of diversity [15]. Hence, even though bit error performance can be improved due to higher diversity gain by employing lower channel coding rates, the overall system performance may be degraded due to the reduction in source coding rate. Hence, for better system performance, the information rate and diversity gain tradeoff becomes an important issue and requires detailed investigation.

Inspired by a recent paper [2] in which the relative effectiveness of application layer diversity techniques and physical layer diversity techniques are compared, we argue that the concept of channel coding across multiple independent components and the use of multiple description coding can sometimes be seamlessly combined to achieve a better system performance. In particular, by considering transmission of a progressive bitstream using an orthogonal frequency division multiplexing (OFDM)[1] system, we develop a cross-layer diversity technique taking advantage of both the application layer and the physical layer diversities. More specifically, based on the order of diversity, we combine the concept of channel coding across independently faded components with the construction of multiple independent descriptions using an FEC-based strategy [11], [18], [19]. As will be demonstrated subsequently, the proposed approach not only gives an improved overall system design, but also provides better insight into the relative effectiveness of transmission schemes using multiple description coding. We provide an analysis of this cross-layer technique and demonstrate the superior performance of this approach using the set partitioning in hierarchical trees (SPIHT) [20] image coder. In this paper, each description is a single packet, so we shall use the terms "description" and "packet" interchangeably throughout the paper.

Some earlier works on multimedia transmission over OFDM networks include Ho and Kahn [21], who studied multimedia transmission over asymmetric digital subscriber lines (ADSL) using a water-filling based technique. However, water-filling based techniques generally result in a large overhead for channel state information (CSI) feedback (as they require feedback of the entire multipath intensity profile) making them most suitable for slowly varying channels. Hence, FEC-based approaches using channel coding across subcarriers are common alternatives in mobile wireless environments [22]. Song and Liu [23] considered progressive image transmission over OFDM systems with multiple antennas using space time block codes. The authors assumed all subcarriers to be independently fading and proposed a joint source-channel rate allocation scheme based on the average signal-to-noise ratio of the wireless channel. Video transmission over space-time coded OFDM systems was also discussed in [17] and [24]. In [25], Xu *et al.* studied the optimal bit allocation method for transmission of an MPEG-4 compressed video stream. Also, Cherriman *et al.* investigated video telephony over an OFDM system employing turbo coding and adaptive modulation [26].

The remainder of this paper is organized as follows: In Section II, we describe some technical preliminaries, including some basics of OFDM systems and FEC-based multiple description coding. In Section III, we give a description of the channel model. In Section IV, we describe the proposed cross-layer diversity approach and discuss some of the associated tradeoff issues. In Section V, we study the packet loss probability mass function for an OFDM system used over a frequency-selective fading channel. In Section VI, we provide some simulation results and discussion. Finally, Section VII gives a summary and conclusions.

II. Preliminaries

A. Orthogonal Frequency Division Multiplexing (OFDM)

Fig. 1 shows the baseband model of a typical OFDM system. The basic principle of OFDM is to split a high-rate data stream into a number of lower rate streams that are transmitted over

[1]The acronym OFDM here refers to coded OFDM systems.

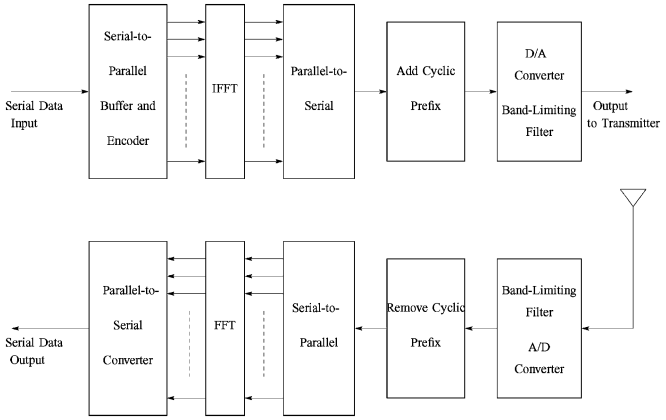

Fig. 1. Baseband OFDM system.

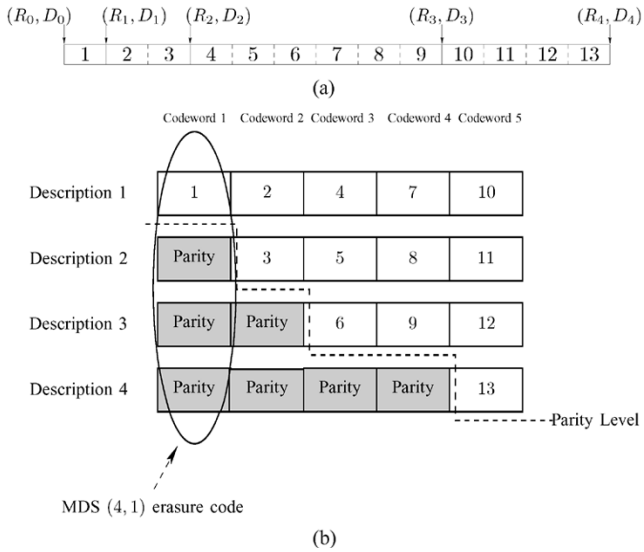

Fig. 2. Illustration of the FEC-based multiple description coding technique for an embedded bitstream with $n = 4$ descriptions. (a) An embedded description from the source coder partitioned into five quality levels of Rate R_g and distortion $D(R_g) = D_g, g = 0, 1, \ldots, 4$. (b) $N = 4$ independent and equally important descriptions.

overlapped but orthogonal subcarriers. Since the symbol duration increases for the lower rate parallel subcarriers, the relative amount of dispersion in time caused by multipath delay spread is decreased. By inserting a guard interval between successive symbols, the problem of intersymbol interference (ISI) can then be reduced. In practice, this means that symbols are transmitted in parallel over a number of frequency-nonselective (flat-fading) channels. To maintain the orthogonality of the subcarriers and avoid intercarrier interference (ICI), a cyclic extension (cyclic prefix) is appended to the beginning of the OFDM symbols. The cyclic prefix is removed at the receiver.

In general, the baseband form of the transmitted signal can be written as

$$s_T(t) = \frac{1}{\sqrt{N_t}} \sum_i \sum_p \sum_{n=0}^{N_t-1} s_{i,n,p} e^{j2\pi nt/T} \Pi(t - pT) \quad (1)$$

where T is the symbol duration including the guard time (T_g), N_t is the total number of subcarriers, $s_{i,n,p}$ is the ith constellation point for the pth symbol on the nth subcarrier, and

$$\Pi(t) \triangleq \begin{cases} 1, & \text{if } 0 < t < T \\ 0, & \text{otherwise.} \end{cases} \quad (2)$$

Due to the frequency-selectivity of the multiple parallel channels, frequency diversity can be exploited by adding redundancy across the subcarriers to combat channel errors due to multipath fading. This can be achieved, for example, by sending signals that carry the same information through different channels so that multiple independently faded replicas of the information symbol can be obtained and a more reliable reception can be achieved. However, in essence, this comes at the expense of a reduced information rate. On the other hand, by transmitting independent data streams in parallel through the independent spectral channels, the information rate can be increased at a price of sacrificing frequency diversity. Hence, there is a tradeoff between the information rate and the diversity gain, which is essentially a tradeoff between the error probability and the data rate of the system. Generally, the maximum achievable diversity gain of an OFDM system is proportional to the number of independently fading channels, N. Note that $N = 1$ corresponds to a flat-fading environment, while $N > 1$ corresponds to a frequency-selective environment. For a flat-fading environment, frequency diversity techniques such as channel coding across the subcarriers are ineffective.

B. FEC-Based Multiple Description Coding

We first provide a brief overview of the FEC-based multiple description coding [11], [18], [27] in which maximum distance separable (MDS) (n, k) erasure codes are used to construct multiple independent bitstreams under a joint source-channel coding framework. An (n, k) erasure code with minimum distance $d_{\min}$ refers to a construction where k information symbols belonging to a finite field are encoded into n channel symbols (belonging to the same finite field) such that the reception of any $(n - d_{\min} + 1)$ of the n channel symbols allows the original k information symbols to be recovered. Channel codes with $d_{\min} = n - k + 1$ are referred to as MDS codes. This implies that the k information symbols can be recovered if any k channel symbols are correctly received. The class of Reed–Solomon (RS) codes is a popular class of codes possessing this property. Based on this property, Mohr *et al.* [11] presented an unequal loss protection framework in which unequal amounts of RS parity symbols are applied to embedded descriptions, and showed that the approach can provide a graceful degradation of delivered image quality as packet losses increase. Later, Puri *et al.* [19] presented a sub-optimal algorithm using Lagrangian optimization principles for the FEC-based multiple description coding. Both papers considered using this approach for multimedia delivery over the Internet. Pradhan *et al.* [28] provided some information-theoretic studies for a Gaussian source.

Fig. 2(a) shows a typical embedded bitstream, in which the source can be reconstructed progressively from the prefixes of the bitstream, while an error generally renders the subsequent bits useless. In Fig. 2(b), we illustrate the general mechanism for converting an embedded bitstream from a source encoder into multiple descriptions in which contiguous information symbols

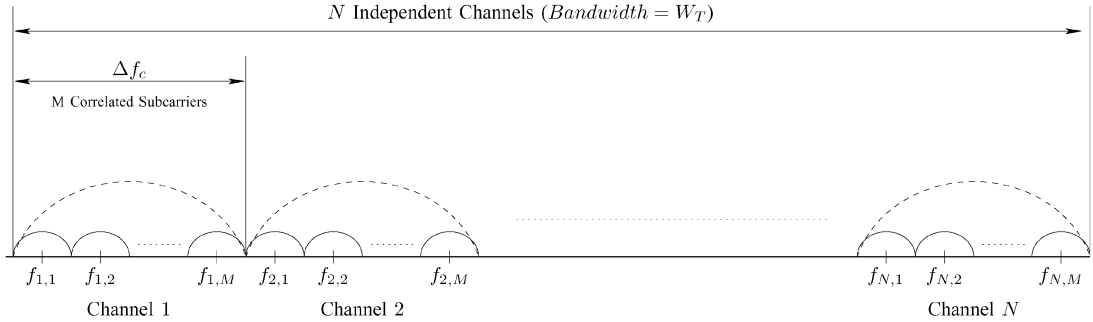

Fig. 3. Subcarrier spectrum assignment.

are spread across the multiple descriptions. The information symbols are protected against channel errors using systematic $(n = 4, k)$ MDS codes, with the level of protection depending on the relative importance of the information symbols. Generally, an (n, k) MDS erasure code can correct up to $n - k$ erasures. Hence, if *any* g out of n descriptions are received, those codewords with minimum distance $d_{\min} \geq n - g + 1$ can be decoded. As a result, decoding is guaranteed at least up to distortion $D(R_g)$, where $D(R_g)$ refers to the distortion achieved with R_g information symbols. For example, in Fig. 2(b), we show the construction of a (4, 1) systematic MDS code (codeword 1) in which erasure of any three descriptions still allows us to reconstruct information symbol 1 and achieve a delivered quality equal to $D(R_1)$. Note that when the source is encoded in a progressive way, using the conventional systematic MDS codes, it is sometimes possible to achieve a fidelity higher than $D(R_g)$ based on the reception of g descriptions. Thus, the distortion measure based on the number of correctly received descriptions essentially represents a lower performance bound on the reception of *any* g descriptions. However, the extra fidelity gain associated with the transmission using an embedded bitstream requires simultaneous successful reception of a small number of particular combinations, rather than any arbitrary combination, of the g received descriptions. If the number of descriptions is large, the probability of a particular combination becomes relatively small. As a result, the lower bound gives a good approximation to the overall system performance. Therefore, in this work, we shall use this approach to evaluate the overall system performance.

III. Channel Model

Consider an OFDM system with spectrum assignment shown in Fig. 3. As illustrated in the figure, we assume a frequency-selective environment, with overall system bandwidth W_T such that we can define N independent channels. Each of the N independent channels consists of M correlated subcarriers spanning a total bandwidth approximately equal to coherence bandwidth, Δf_c. As a result, the total number of subcarriers in the OFDM system considered here is equal to $N_t = N \times M$. Since Δf_c is greater than or equal to the signal bandwidth of an individual subcarrier, each subcarrier is assumed to experience flat-fading. In the time domain, we assume the channel experiences slow Rayleigh fading (i.e., the channel symbol duration is much smaller than the coherence time) such that the fading coefficients are nearly constant over a packet. Since the Doppler spread and delay spread for each subcarrier are approximately the same, we can further assume that the N individual channels are independent and identically distributed (i.i.d.).

Let $s[n, u, v]$ be the vth input modulated symbol of a description at the uth subcarrier in the nth channel. Let the block length of a description be denoted as V, in terms of the number of modulated symbols. At the receiver end, the output signal $r[n, u, v]$ can be expressed as

$$r[n,u,v] = \alpha[n,u,v]s[n,u,v] + w[n,u,v] \quad n \in [1,N], u \in [1,M], v \in [1,V] \tag{3}$$

where $w[n, u, v]$ is a zero-mean complex Gaussian random variable with independent in-phase and quadrature-phase components and identical variance σ^2. We also assume that $w[n, u, v]$ is independent for different n's, u's and v's. Due to the highly correlated nature of the subcarriers within a channel, we have

$$\alpha[n,u,v] \approx \alpha[n,v] \tag{4}$$

where α is a zero-mean complex valued Gaussian random variable with Rayleigh-distributed envelope. This corresponds to the widely used block fading approximation in the frequency domain [29]–[32]. This model is widely used to study the behavior of mobile wireless communication systems due to its simplicity and its ability to provide a good approximation to actual physical channels.

IV. Cross-Layer Diversity Technique and Some Tradeoff Issues

A. System Description and Problem Formulation

In this section, we describe the proposed coding scheme using the adaptive cross-layer approach combining application layer and physical layer diversity techniques. In order to illustrate the basic ideas, we only consider frequency diversity techniques achieved by coding across the subcarriers using the class of MDS Reed-Solomon (RS) codes, without considering time diversity or space diversity techniques. Generally, due to the bursty nature of the errors associated with a slow-fading environment [33] (as considered in this paper), time diversity techniques using channel coding plus intra-packet interleaving become less effective [34].

As illustrated in Fig. 4, based on the total number of subcarriers (N_t) of an OFDM system, an embedded bitstream is first converted into $N_t = N \times M$ approximately equally important descriptions using the FEC-based multiple description coder

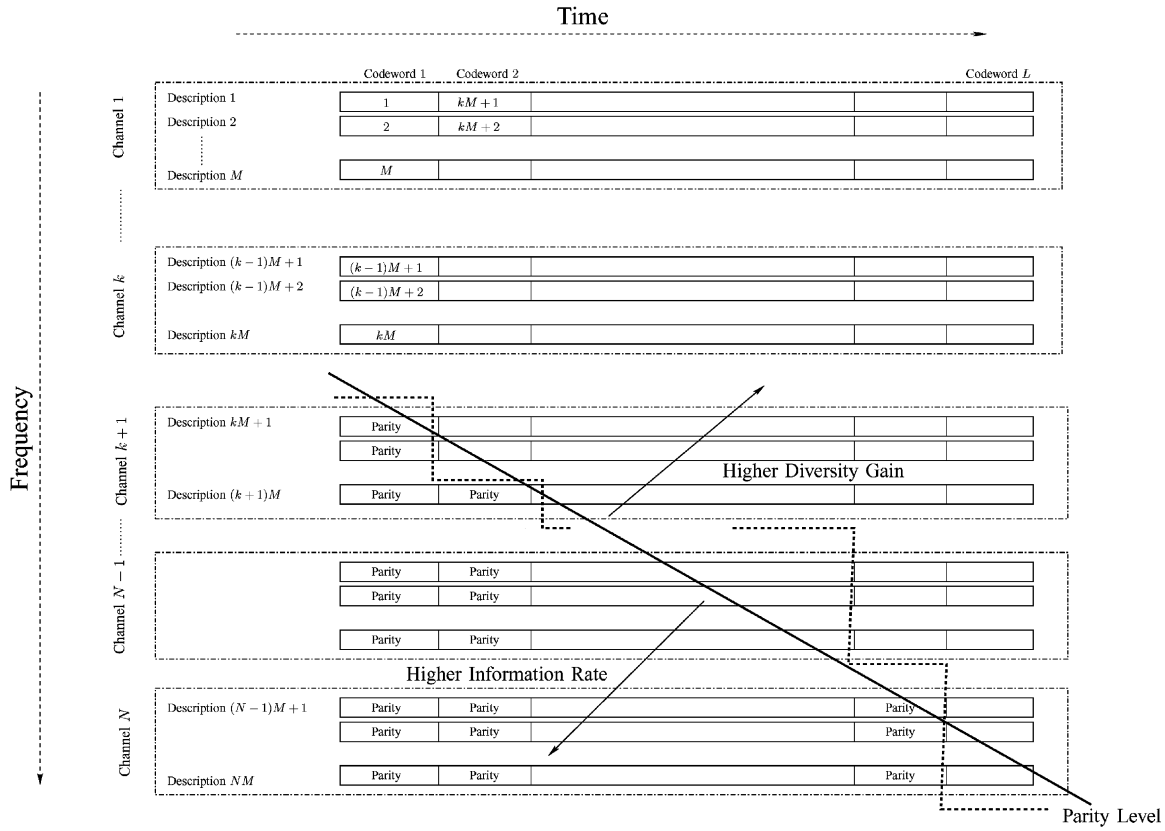

Fig. 4. Proposed cross-layer diversity coding scheme.

[11], [18], [19], where N is the total number of independent channels and M is the number of correlated subcarriers. As discussed in the last paragraph in Section II-B, the N_t descriptions are not exactly equally important, but by treating them as such, we will get a tight lower bound on the overall system performance. The multiple description image/video encoder chooses unequal error protection using the RS codes based on the rate-distortion curve of the source, the channel conditions, and the degree of diversity available at the physical layer. In this work, each code symbol consists of 8 bits or, equivalently, four QPSK symbols. Two bytes of a cyclic redundancy check (CRC) code are appended to each description for error detection. The $N_t = N \times M$ independent descriptions are then mapped to the N_t subcarriers and transmitted through the OFDM system. Due to the individually decodable nature of multiple description coding techniques, if any of the subcarriers/channels are under deep fades and lost, the source can still be recovered from other correctly received subcarriers with a fidelity depending on the number of correctly received descriptions.

Following the standard formulation of the FEC-based multiple description coding [11], [19], [35]–[37], the optimization problem can be described as follows. Given N i.i.d. channels, each with M subcarriers and packet size equal to L code symbols,[2] we assume that for codeword l, c_l code symbols are assigned to information symbols. Hence, the number of parity symbols assigned to codeword l is

$$f_l = N_t - c_l \quad l \in [1, L]. \tag{5}$$

[2]Since each code symbol contains 4 modulated symbols, the packet size in terms of modulated symbols is $V = 4 \times L$.

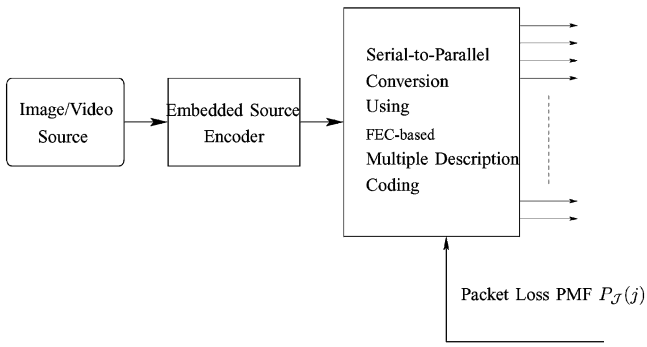

Fig. 5. Block diagram for the proposed OFDM system.

Let ϕ_{th} be the minimum number of descriptions that a decoder needs to reconstruct the source and g be the number of correctly received packets. The reception of any number of packets $g \geq \phi_{\text{th}}$ leads to improving image/video quality $D(R_g)$, where R_g is the information rate, in terms of the number of MDS symbols

$$R_g = \sum_{\{l: c_l \leq g\}} c_l. \tag{6}$$

Hence, the overall channel coding rate equals $R_c = (R_{N_t} + R_{\text{CRC}})/(N_t \times L)$, where R_{CRC} is the bit budget, in terms of the number of MDS symbols, for CRC codes. Given the operational rate-distortion curve $D(R_g)$ and the packet loss probability mass function $P_{\mathcal{J}}(j)$, where j is the number of lost

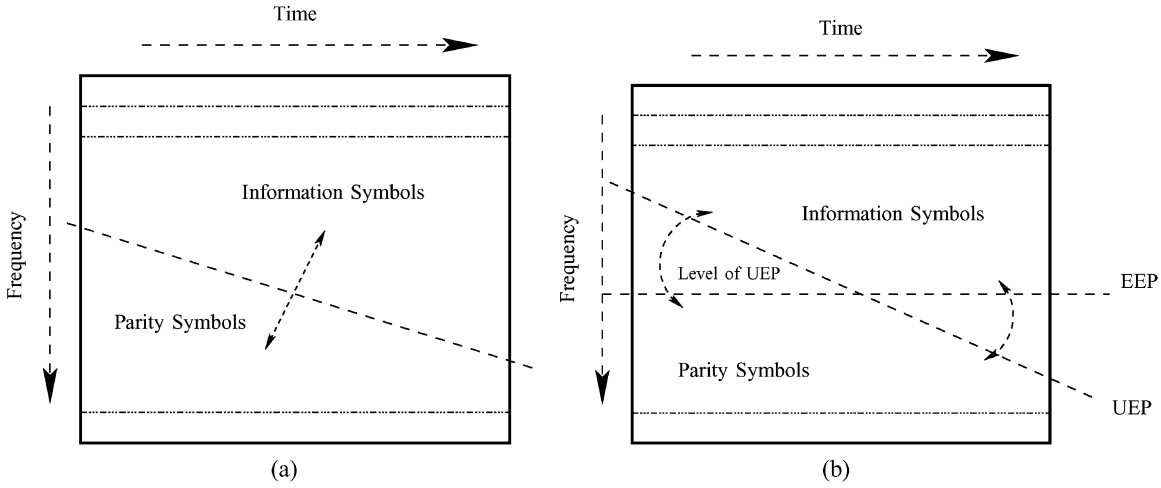

Fig. 6. Tradeoff issues associated with the cross-layer diversity technique. (a) Parity level and (b) degree of unequal error protection.

packets such that $j = N_t - g$, we can then minimize the expected distortion

$$E^*[D] = \min_{\{c_l\}} \left\{ \sum_{j=0}^{N_t-\phi_{\rm th}} P_{\mathcal{J}}(j) D(R_{N_t-j}) + \sum_{j=N_t-\phi_{\rm th}+1} P_{\mathcal{J}}(j) D_0 \right\} \quad (7)$$

where D_0 corresponds to the distortion when less than ϕ_{th} descriptions are received and so the decoder must reconstruct the source without being able to use any of the transmitted information. For a still image, this typically means reconstructing the entire image at the mean pixel value.

Fig. 5 shows the block diagram for the proposed OFDM system using the cross-layer diversity transmission scheme. It should be noted that while the rate-distortion function $D(R_g)$ is readily available at the transmitter, only the receiver has the knowledge of N, M, and $P_{\mathcal{J}}(j)$. Nevertheless, we assume that the information can be passed from the receiver to the transmitter through a reliable feedback channel. The transmitter uses $D(R_g)$ together with these three parameters to compute the c_l values. We also assume that the side information regarding c_l can be transmitted reliably to the receiver.

Different algorithms can be used to find the allocation of parity symbols for the optimization problem. A local iterative search algorithm was introduced in [11] by Mohr *et al.* with the quality of the solution depending on a search parameter Q in which $2QL$ different possible assignments were examined in each iteration. Hence, the running time is $O(QL)$ per iteration. In [38], Mohr *et al.* proposed a faster, approximately optimal, assignment algorithm with complexity $O(hN_t \log N_t)$, where h is the number of vertices on the convex hull of the operational rate-distortion function. Puri *et al.* [27] provided a Lagrangian multiplier-based suboptimal solution. The running time of the Lagrangian optimizer is $O(N_t)$ per Lagrangian multiplier tested. In [37], Stockhammer *et al.* presented an optimal solution with complexity $O(N_t^2 L^2)$ using a dynamic programming algorithm, provided the operational rate-distortion function is convex and the packet loss probability is a monotonically decreasing function of the number of lost packets. Dumitrescu *et al.* [36] gave an $O(N_t^2 L^2)$ algorithm that is optimal in the general case. However, they showed that the optimization algorithm can be reduced to $O(N_t^2 L)$, provided that the operational rate-distortion function is convex. A simpler local search algorithm with complexity $O(N_t L)$ was presented in [35]. The algorithm supports realtime optimization and produces good results in general. For the cases of approximately 100–200 packets, all of the above approaches give approximately the same results [35]. In this paper, we are interested in the construction of FEC-based multiple description coding taking into consideration the order of diversity at the physical layer. Therefore, we use the approach proposed in [11] due to its simplicity. We set $Q = N_t$ for a full search.

B. Some Tradeoff Issues

As we have mentioned previously, for an OFDM system employing frequency diversity techniques, there is a tradeoff between the information rate and the diversity gain. In essence, this is the tradeoff between the error probability and the data rate of the system. As illustrated in Fig. 6(a), the symbols above the boundary (dashed line) are the information symbols, while those symbols below the boundary are parity symbols. Hence, the boundary corresponds to the level of parity used. By moving the boundary upwards, more redundancy is added across the subcarriers. As a result, a higher diversity gain, and hence smaller error probability, is achieved at a reduced information rate. This tradeoff is particularly important for certain image/video transmission methods, as the output bitstream after compression may be extremely sensitive to channel errors and sometimes a single bit error may render the entire source unrecoverable.

In addition to the tradeoff between the information rate and diversity gain, the degree of unequal error protection (UEP) is another important issue associated with multimedia transmission over the OFDM system. Generally, as the compressed bitstream from an image/video encoder has different sensitivities toward channel errors, it is expected that the overall system performance can be significantly improved by employing UEP techniques. In particular, by adding additional redundancy to the more important bits and less redundancy to the less important

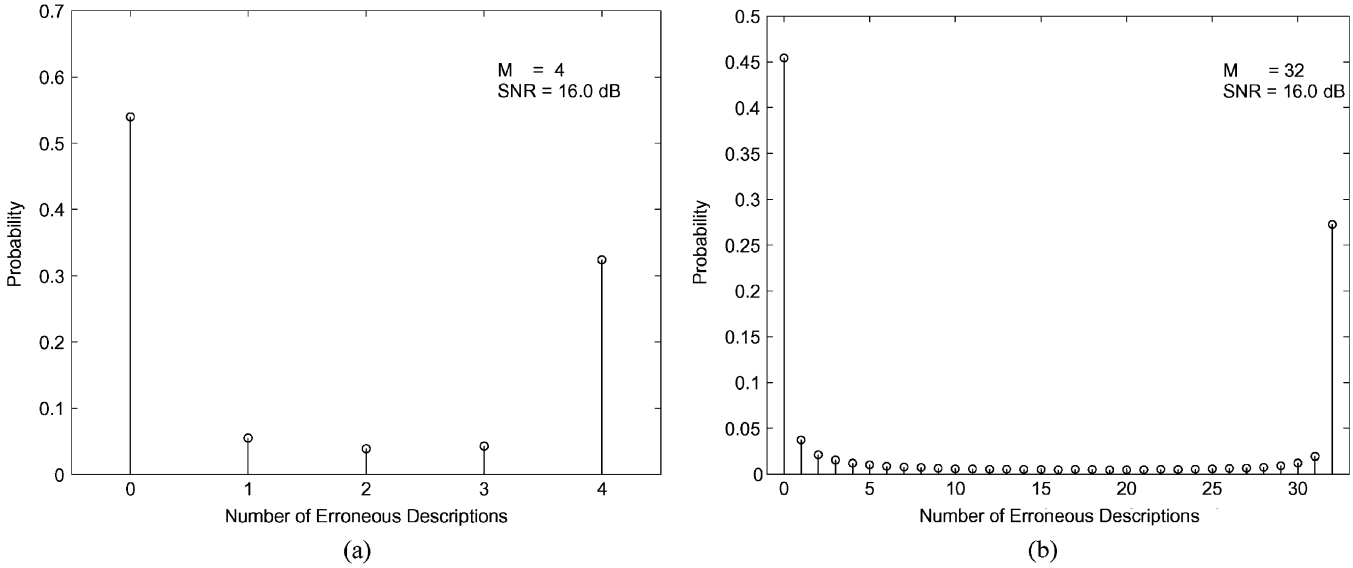

Fig. 7. Packet loss probability mass function (PMF) $P_{\mathcal{M}}(m)$ for a single channel with different coherence bandwidths and hence different numbers of correlated subcarriers, M. (a) $M = 4, \mathrm{SNR} = 16.0$ dB. (b) $M = 32, \mathrm{SNR} = 16.0$ dB.

bits, subject to a constraint on the overall bit budget, the performance of the system can be greatly enhanced. For the system considered here, since the relative importance of an embedded bitstream is strictly decreasing, this results in a tilted boundary across the subcarriers, as illustrated in Fig. 6(b), which corresponds to a decreasing level of parity protection for the codewords on the right. The gradient of the boundary indicates the degree of UEP required for optimal performance. A horizontal boundary represents an equal error protection (EEP) strategy.

It should be noted that, for an EEP transmission scheme, we can also optimize the number of parity symbols by raising or lowering the horizontal parity boundary based on the degree of diversity at the physical layer. We refer to this as adaptive EEP. Regardless of what level one picks, however, the EEP transmission schemes can be considered to correspond to the transmission of a *single description* over an OFDM system. If (n, k) MDS erasure codes are used, the reception of any $g \geq k$ out of n packets allows the decoder to reconstruct the source at the same particular distortion level D', while the reception of $g < k$ packets renders the entire source unrecoverable (distortion D_0). As there is only one possible distortion level that can be achieved (other than the zero-information quality level D_0), we do not consider this as multiple description coding. Hence, our study of the EEP transmission is useful from two points of view. First of all, it is of interest to optimally trade off diversity gain and information rate by choosing the level of EEP coding. Secondly, our UEP approach is a cross-layer diversity scheme in which both the physical layer diversity and application level diversity (multiple description coding) are being jointly exploited. The EEP system serves as a comparison system in which the physical layer diversity is still being exploited, but the application layer diversity has been removed.

V. Packet Loss Probability Mass Function

As indicated in (7), the optimal allocation of the c_l and $f_l, l \in [1, L]$, and hence the delivered image/video quality, depends on the packet loss probability mass function (PMF) $P_{\mathcal{J}}(j)$, where $j \in [0, N_t]$ is the number of packets lost. Although the PMF can be found analytically for uncorrelated fading channels, due to the correlated fading in both the time and frequency domains of the wireless environment considered here [39], we use simulation to find the packet loss PMF. Specifically, we use the modified Jakes' model which has been shown to yield accurate results for Rayleigh fading channels [40] to simulate the fading coefficient $\alpha[n, u, v]$ in (3). We assume ideal coherent detection in our simulations. In Fig. 7(a), we show the packet loss PMF $(P_{\mathcal{M}}(m), m \in [0, M])$ for a single channel in which the coherence bandwidth (Δf_c) spans a bandwidth equal to $M = 4$ correlated subcarriers. The size of the packet (V) is equal to 256 QPSK symbols (i.e., 512 bits). The normalized Doppler spread (f_{nd}) (i.e., the Doppler spread normalized by the channel symbol rate) is set to be 10^{-3}, and the signal-to-noise ratio (SNR) is set to 16.0 dB. As shown in the figure, for a single channel, the packets are likely to be either all correctly received $(m = 0)$ or corrupted simultaneously $(m = 4)$. The results can briefly be explained by considering the 2-state Gilbert-Elliot channel model, which was shown to be accurate for data transmission over fading channels for a broad range of parameters [33]. In the good state, the fading coefficients $\alpha[n, u, v]$ are enhanced by constructive addition. Therefore, all the packets are likely to be correctly received. In the bad state, the correlated carriers suffer deep fades at the same time. Hence, the packets are likely to be corrupted simultaneously. Similarly, in Fig. 7(b), we show the packet loss PMF for a single channel with $M = 32$. As expected, we have $m = 0$ or $m = 32$ being the most probable events. We provide a more detailed analysis in Appendix A.

To obtain a better understanding of the effects of the coherence bandwidth and the order of diversity on the system performance, we show some simulation results on $P_{\mathcal{J}}(j)$ using the block fading channel model. It should be noted that the block fading channel model is a simplified model. In reality, the channel responses may fluctuate across the subcarriers in a more random manner. Nevertheless, the model has been shown to

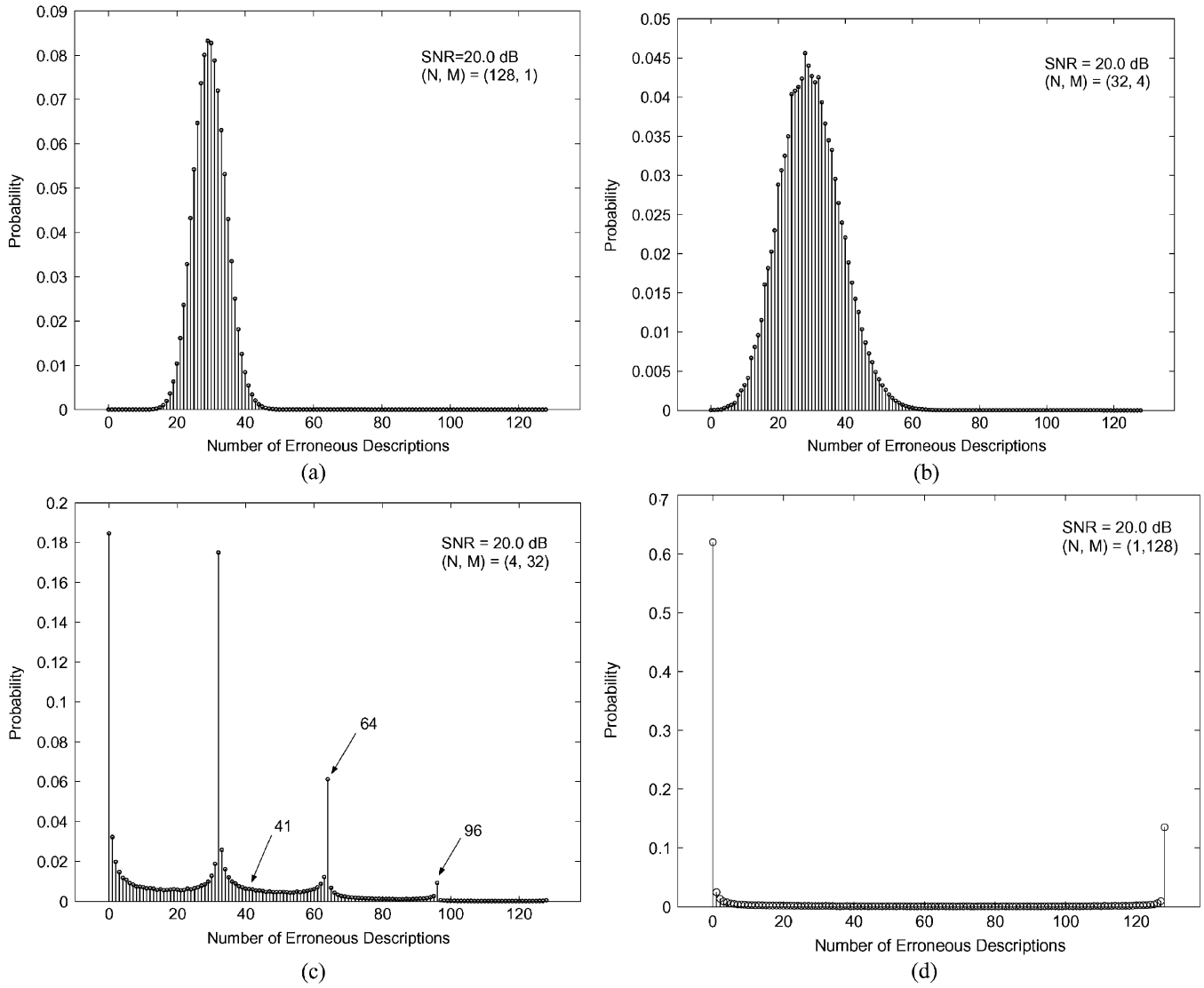

Fig. 8. Packet loss PMF for the OFDM system ($N_t = 128$) with different coherence bandwidths and hence different numbers of independent channels N and correlated carriers M. (a) $N = 128, M = 1$. (b) $N = 32, M = 4$. (c) $N = 4, M = 32$. (d) $N = 1, M = 128$.

provide a good approximation to the physical channel, while simultaneously maintaining its analytic tractability [29]–[32]. Here, we consider an OFDM system with $N_t = N \times M = 128$. Again, we have $f_{nd} = 10^{-3}$, and the packet size $V = 256$ QPSK symbols. The SNR is set equal to 20.0 dB. In Fig. 8, we illustrate the effects of N and M on the packet loss PMF $P_{\mathcal{J}}(j)$. Note that, except for the coherence bandwidth (Δf_c), all the other parameters used in the simulations are the same. Thus, the average packet loss probabilities are the same in all the cases considered. Fig. 8(a)–8(d) shows $P_{\mathcal{J}}(j)$ for the systems with $(N, M) = (128, 1), (32, 4), (4, 32)$, and $(1, 128)$, respectively. Due to the effect of correlated fading across the subcarriers, the PMF shows local maxima at integral multiples of M when the number of independent channels is relatively small. For example, in Fig. 8(c), we show a system with $N = 4$ and $M = 32$. As can be seen, $P_{\mathcal{J}}(j)$ is relatively high at $j = 0, 32, 64, 96$, and 128. In the extreme case, as presented in Fig. 8(d), we have $N = 1$ and $M = 128$, which represents a flat-fading environment. In such a circumstance, it is likely that either all of the 128 subcarriers are received correctly or lost simultaneously. It can also be noticed that the variance of the number of packet losses, j, decreases as N increases. In particular, the packet loss PMF $P_{\mathcal{J}}(j)$ for the system with $N = 128$ [Fig. 8(a)], having the largest number of independent channels, has the smallest variance. Further discussion can be found in Appendix B. We thus see that the physical layer diversity has a tremendous impact on the PMF $P_{\mathcal{J}}(j)$. Hence, any efficient coding schemes should take it into consideration for better system performance.

VI. Results and Discussion

We carried out simulations on the 512×512 gray-scale images Lena, Peppers, and Goldhill. Similar results were obtained for all three. Hence, in this paper, we only present the results using the Lena image. The image was encoded using the SPIHT [20] algorithm to produce an embedded bitstream. The serial bitstream was converted to 128 parallel bitstreams using the FEC-based multiple description encoder. The 128 descriptions were mapped to the OFDM system with 128 subcarriers. We used RS codes for error protection, and there were 8 bits per RS

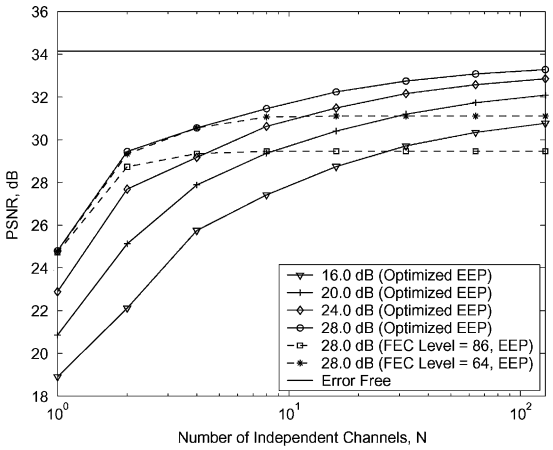

Fig. 9. Optimized PSNR versus Number of independent channels (N) for the adaptive cross-layer OFDM system employing EEP techniques under different SNRs.

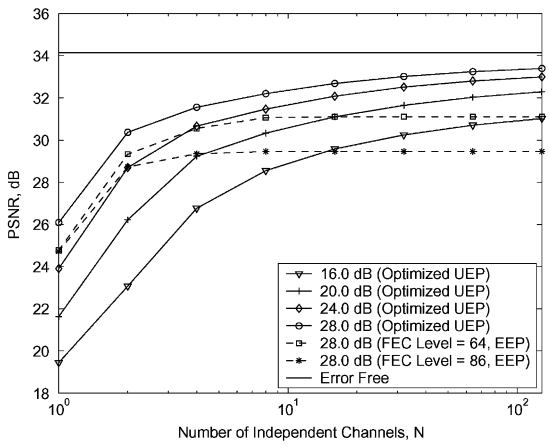

Fig. 10. Optimized PSNR versus Number of independent channels (N) for the adaptive cross-layer OFDM system employing UEP techniques under different SNRs.

symbol. The packet size was set equal to 512 bits, corresponding to 64 RS symbols.

In Fig. 9, we illustrate the importance of the information rate and diversity gain tradeoff. In particular, we show the optimal peak-signal-to-noise ratio (PSNR)[3] performance versus the number of independent channels, N, employing the adaptive EEP techniques. The performance is optimized by raising or lowering the parity line based on N. We show the results for $\mathrm{SNR} = 16.0$, 20.0, 24.0, and 28.0 dB, corresponding to average packet loss rate $(\mathrm{PLR}) = 36\%$, 21%, 11%, and 6%, respectively. As expected, for a fixed total number of subcarriers $N_t = 128$, as N increases, there is a significant improvement in overall system performance measured in terms of PSNR, even though the average PLRs are the same. Note that the PSNR increases monotonically as N increases. Note also the relatively poor performance for the frequency diversity technique in a flat-fading environment $(N = 1)$. In Fig. 9 we also plot the PSNR performance for systems without employing the adaptive strategy. In particular, we fix the coding levels at $f_l = 64$ and $f_l = 86, \forall l \in [1, L]$ (corresponding to overall channel coding rates $R_c = 1/2$ and $R_c = 1/3$), respectively, without taking into consideration the number of independent channels available at the physical layer. It can be noticed that the PSNR performances of both systems improve as the number of independent channels increases due to higher diversity gains. However, the rate of improvement diminishes quickly. As shown in the figure, only marginal improvement can be achieved beyond $N = 4$ for $f_l = 64$, while no further practical gain can obtained for $f_l = 86$ beyond $N = 4$. For the purpose of comparison, in the figure, we also include a plot of the PSNR performance for error-free channel conditions.

In Fig. 10, we show the optimal PSNR versus the number of independent channels for the adaptive cross-layer diversity approach employing UEP techniques for different SNRs. Again, we show the results for $\mathrm{SNR} = 16.0$, 20.0, 24.0, and 28.0 dB, corresponding to average $\mathrm{PLR} = 36\%$, 21%, 11%, and 6%, respectively. For a fixed number of total subcarriers $N_t = 128$,

[3] $\mathrm{PSNR} \triangleq 10 \log \frac{255^2}{\mathrm{MSE}_{\mathrm{avg}}}$.

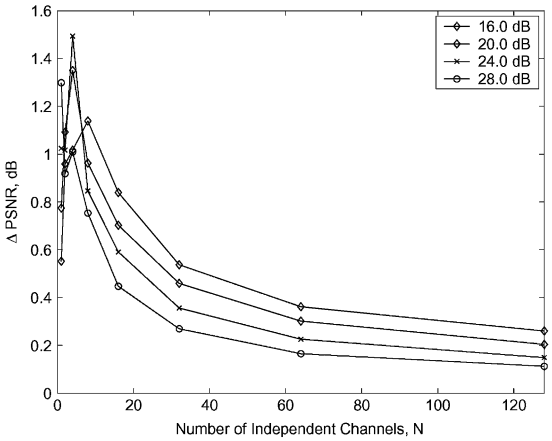

Fig. 11. Difference in optimized PSNR performance between unequal error protection (UEP) and equal error protection (EEP) versus the number of independent channels N.

the overall system performance measured in terms of PSNR improves monotonically as the number of independent channels increases. For comparison, we also include plots of the PSNR performance for error free channel conditions, as well as for the systems using fixed parity levels with $f_l = 64$ and $f_l = 86$. Observe, in particular, the optimized UEP schemes generally give a larger performance gain than the optimized EEP schemes.

In Fig. 11, we show the difference in the PSNR performance between the optimized UEP and optimized EEP strategies versus N. As can be seen, there is a significant improvement in the PSNR performance by employing the optimized UEP technique, in particular, when N is small. Generally, a larger performance gain is achieved at the lower SNRs, corresponding to poorer channel conditions. Note that the advantage of the optimized UEP strategy relative to EEP diminishes with increasing N. As discussed previously, the variance of packet losses, j, decreases with increasing N, thus reducing the need and hence the relative advantages of the UEP techniques. Nevertheless, in some OFDM systems, the number of independent channels N might be limited. Hence, there is a significant advantage in employing our proposed cross-layer diversity and UEP techniques. In Fig. 12, we show

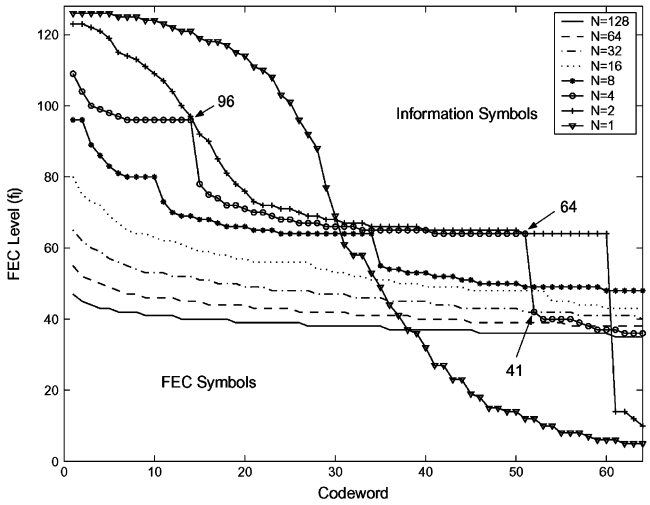

Fig. 12. Profiles showing the optimal allocation of source and channel symbols for systems with different numbers of independent channels N.

TABLE I
STATISTICS FOR THE OPTIMUM PARITY LEVEL f_l FOR $\mathrm{SNR} = 20.0$ dB

No. of Indep. Channels (N)	Mean μ_{f_l}	Std. Dev. σ_{f_l}
128	38.38	2.64
64	42.23	3.85
32	47.36	5.66
16	54.01	8.56
8	61.61	12.84
4	67.95	19.91
2	74.76	25.32
1	65.12	48.42

the optimal allocation of the information symbols and parity symbols for $\mathrm{SNR} = 20.0$ dB, with average PLR approximately equal to 21%. In particular, we present the boundaries, given by f_l in (5), for systems with different N, and hence different potential diversity gains. The symbols above the boundaries are the information symbols, while those below the boundaries are the RS parity symbols. As can be seen, since the relative importance of an embedded bitstream is strictly decreasing, less redundancy is added across the subcarriers as we move to the right. Further analysis of the boundaries is provided in Table I, where we show the mean and standard deviation of f_l. Generally, as N increases, the average parity level decreases. (There is an exception for $(N, M) = (1, 128)$, mainly due to the ineffectiveness of frequency diversity techniques in a flat-fading channel.) This indicates that as N increases, less redundancy needs to be added across the subcarriers for optimal system performance.

Moreover, the degree of UEP, represented by the tilt of the boundary, also increases as N decreases. To provide a specific comparison, consider the cases when $N = 128$ and $N = 2$. The numbers of correlated subcarriers per channel are $M = 1$ and $M = 64$, respectively. For $N = 128$, the standard deviation of f_l equals 2.64 and the number of parity symbols ranges from $f_1 = 47$ for the most important information symbol to $f_{64} = 35$ for the least important information symbol. For $N = 2$, the standard deviation of f_l is 25.32 and the number of parity symbols ranges from $f_1 = 123$ for the most important information symbol to $f_{64} = 10$ for the least important information symbol. As indicated in the plots and discussions for the packet loss PMF, $P_{\mathcal{J}}(j)$, in the previous section, as N increases, the variance of the number of packet losses, j, decreases and thus reduces the degree of UEP. It can also be noticed that the boundary exhibits a stepwise behavior when N is small. This is mainly due to the highly correlated fading within a channel, which results in the loss of correlated subcarriers simultaneously when a channel is under a deep fade. For example, consider the case when $(N, M) = (4, 32)$. The corresponding packet loss PMF $P_J(j)$ is shown in Fig. 8(c), and exhibits local maxima at integral multiples of $M = 32$, i.e., $j = 0, 32, 64, 96$. From the plot of the boundary in Fig. 12 for $N = 4$, we notice that the most important information symbols are protected against $j = 96$ with $f_l \geq 96$. The relatively less important information symbols are protected against $j = 32$ and $j = 64$, with $f_l \geq 64$ and $f_l \geq 32$, respectively.

Generally, frequency diversity techniques that add redundancy across spectral subcarriers are ineffective in flat-fading channels $(N = 1)$. This is because it is highly probable that all the subcarriers are either correctly received or corrupted at the same time, as seen previously in Fig. 8(d). This is also indicated by the relatively poor performance in terms of PSNR for the system, as shown in the subsequent plots. As can be seen from the boundary for $N = 1$ in Fig. 12, except for the relatively strong protection against channel errors for the first few important symbols, there is very little protection for most of the subsequent, less important, symbols.

We compare the performance of this cross-layer diversity approach with the progressive approach proposed in [23]. In [23], the authors consider the progressive transmission of digitally compressed images over an OFDM based system. Just as with the cross-layer approach discussed in this paper, the authors use SPIHT as the source coder. At the system level, the authors also consider an OFDM system with 128 subcarriers[4] using QPSK modulation. For channel coding, both approaches consider RS coding across subcarriers with each RS code symbol consisting of 4 QPSK symbols.[5] However, while both approaches consider spreading the contiguous information bits across the subcarriers, and both use 16-bit CRC codes for error detection, the packets are constructed in a different manner. In particular, in [23], each packet contains one RS codeword in conjunction with a CRC outer code. Hence, the progressive scheme is similar to the approach studied in [41], in which the delivered performance depends on the number of the correctly received packets before the first erroneous packet. The optimal allocation of RS information symbols and parity symbols is solved by the dynamic programming approach developed in [41], based on the assumption that each subchannel is independently faded. Furthermore, the authors of [23] use the expected number of successfully received

[4]In [23], eight subcarriers are used as guard tones. Here, for the purpose of comparison, all 128 subcarriers are used for transmission.

[5]In [23], the 4 QPSK symbols of the same RS code symbol are spread across 4 subcarriers. Hence, for a total of 128 subcarriers, there are 32 RS code symbols per RS codeword.

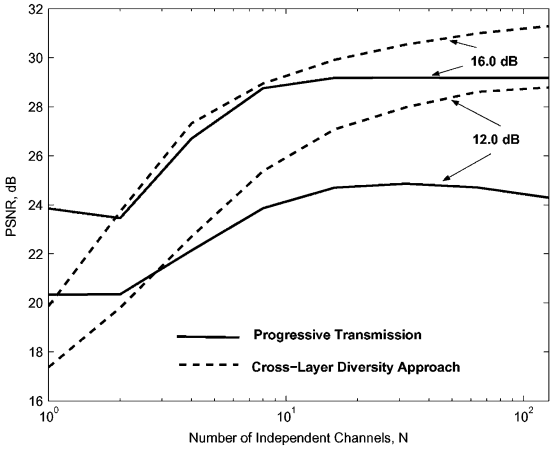

Fig. 13. Optimized PSNR performance for the cross-layer diversity scheme versus the progressive transmission scheme with different numbers of independent channels, N.

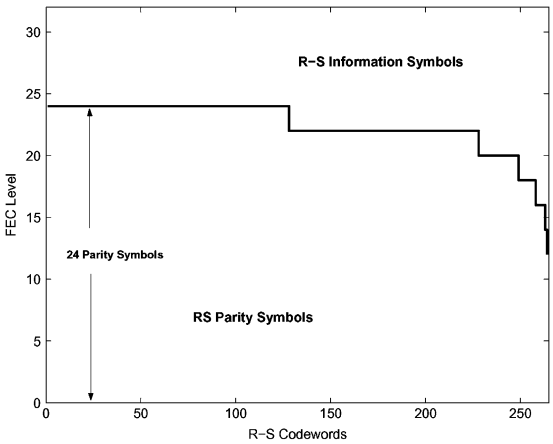

Fig. 14. Profile showing the optimal allocation of RS information and parity symbols for the progressive transmission scheme at $\mathrm{SNR} = 16.0$ dB.

information bits as the optimization criterion. Here, for the purpose of comparison, we use the mean-square error as the criterion for the optimization problem, since it gives better results than maximizing the expected number of successfully received information bits [41].

In Fig. 13, we show the PSNR performance for the proposed adaptive cross-layer diversity approach versus the progressive transmission scheme studied in [23] at SNR of 12.0 and 16.0 dB. As shown in the figure, the cross-layer diversity approach outperforms the progressive approach except when the order of diversity available at the physical layer is small. Intuitively, as stated previously, in order to achieve a satisfactory performance, the use of multiple description coding techniques requires channels which are not highly correlated. Hence, without the availability of independent channels at the physical layer, the performance of multiple description coding could be unsatisfactory.

As can also be observed from the figure, the systems with higher order of diversity generally outperform the systems with lower order of diversity in both approaches, except when the number of independent channels $N = 2$, which is worse than expected. This can be explained as follows. In Fig. 14, we show the optimal assignment of RS information symbols and parity symbols at $\mathrm{SNR} = 16.0$ dB. As indicated in the figure, the number of parity symbols for the most important codewords is 24. Hence, the error correcting capability of the RS codewords is 12. For $N = 2$, the coherence bandwidth spans approximately 64 subcarriers, corresponding to 16 RS code symbols. Hence, if either one of the two correlated channels is experiencing a deep fade, the number of erroneous symbols would be approximately 16, which is greater than the error correcting capability of the RS codewords carrying the most important information. As a consequence, the codewords cannot be corrected in such circumstances. Assume P_g is the probability that a channel is in the good state. For $N = 1$, the probability that the channel is in the good state is P_g. For $N = 2$, the probability that both channels are in the good state is P_g^2, which is smaller than P_g. Hence, the delivered PSNR performance of $N = 2$ is worse than $N = 1$. For $N = 4$, the coherence bandwidth spans approximately 32 subcarriers, corresponding to 8 RS code symbols. Hence, if one of the channels is experiencing a deep fade, the most important codewords can still be recovered using the particular coding scheme shown in Fig. 14. In fact, with the same approximation as shown above, it can be shown that if $P_g > 1/3$, the PSNR performance of $N = 4$ will always better be than that of $N = 2$. Finally, in order to further illustrate the advantages of this cross-layer diversity technique, in Fig. 15, we plot the cumulative distribution functions (CDF) of the PSNR performance for systems with different numbers of independent channels, using both the optimized UEP and the optimized EEP approaches. In Fig. 15(a)–(d), we show the CDFs for systems with $\mathrm{SNR} = 20.0$ dB and $(N, M) = (1, 128), (2, 64), (4, 32), (8, 16)$, respectively. To provide a specific performance comparison, consider, for example, Fig. 15(a). It can be noticed that the optimized UEP approach provides approximately a 2.3 dB gain over the optimized EEP approach with a probability equal to 0.71. Although there are regions over which the optimized UEP approach performs worse than the optimized EEP approach, the probability of that amount is relatively small (about 0.09). The UEP technique also enables the source to be reconstructed under noisier channel conditions than the EEP technique, even though at a low fidelity. From the figure, it can be noticed that the probability that the source cannot be recovered is 0.20 when the optimized EEP technique is used, while the corresponding probability is only 0.14 using the UEP approach.

Similar observations can be found in other systems. Consider, for example, Fig. 15(c), where we illustrate the CDF of a system with $(N, M) = (4, 32)$ at $\mathrm{SNR} = 20.0$ dB. As can be seen, a performance gain of about 2.1 dB can be achieved 94% of the time, while only sacrificing a little performance loss 6% of the time. As stated previously, generally, a higher performance gain can be achieved at lower SNRs, as shown in Fig. 11. This is further illustrated in Fig. 15(e) and (f). In these figures, we show the CDFs of the system at $\mathrm{SNR} = 16.0$ dB with $(N, M) = (1, 128)$ and (2,64), respectively. A 3.1- and a 1.7-dB improvement can be achieved with probabilities 0.57 and 0.79, respectively.

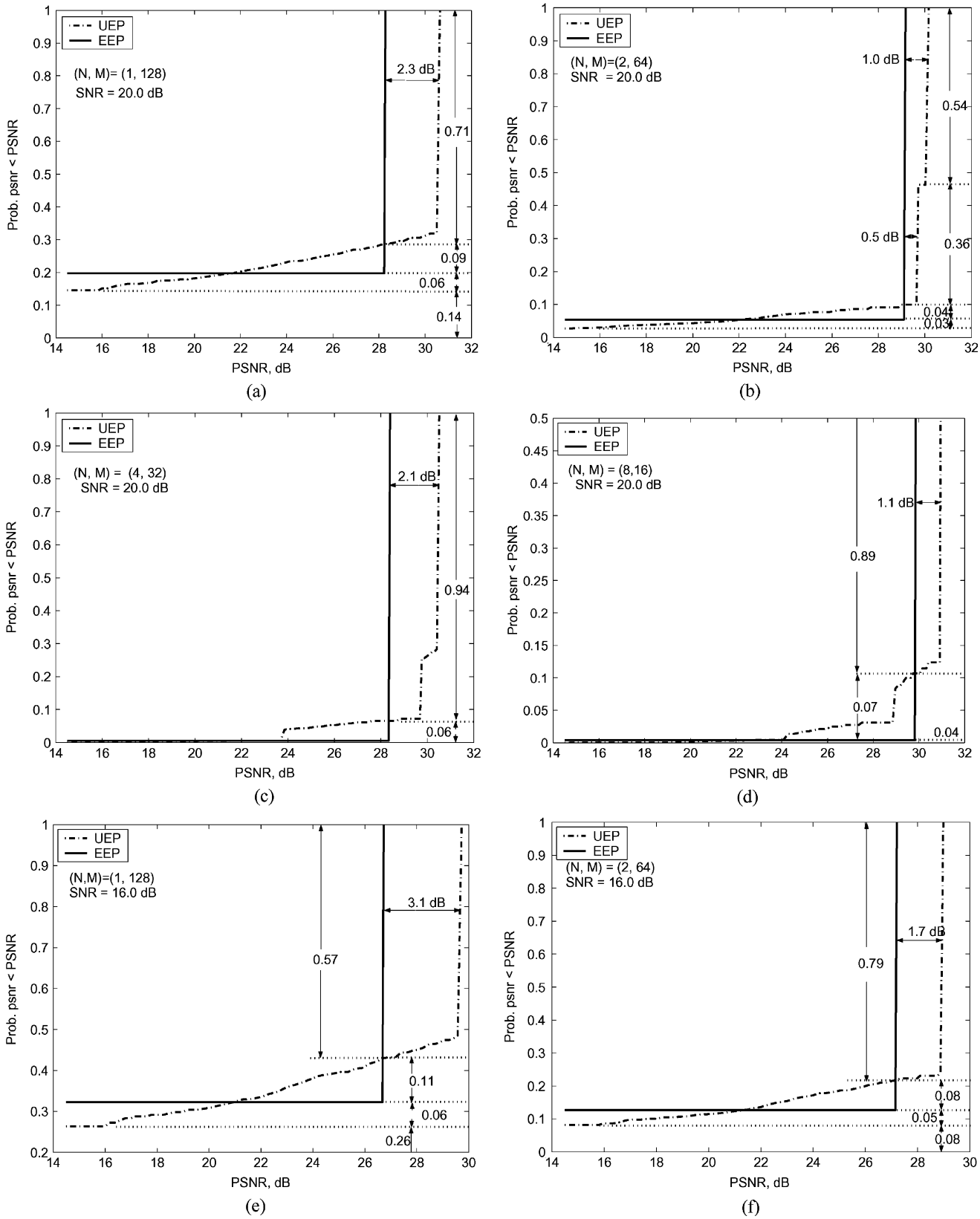

Fig. 15. Cumulative distributions of the optimized PSNR performance for the systems employing UEP and EEP techniques, respectively. (a) $N = 1, M = 128, \mathrm{SNR} = 20.0$ dB. (b) $N = 2, M = 64, \mathrm{SNR} = 20.0$ dB. (c) $N = 4, M = 32, \mathrm{SNR} = 20.0$ dB. (d) $N = 8, M = 16, \mathrm{SNR} = 20.0$ dB. (e) $N = 1, M = 128, \mathrm{SNR} = 16.0$ dB. (f) $N = 2, M = 64, \mathrm{SNR} = 16.0$ dB.

VII. Conclusion

We studied an OFDM system supporting multimedia communications. In particular, assuming a slowly varying Rayleigh fading environment, we investigated the packet loss probability mass function for an OFDM system with different coherence bandwidths, and hence different numbers of correlated subcarriers. We then proposed a cross-layer diversity transmission scheme incorporating both physical layer and application layer diversity. More specifically, based on the frequency selectivity of the OFDM system, we constructed multiple descriptions employing an FEC-based approach. We demonstrated the superior performance of this adaptive cross-layer approach using the SPIHT image coder. We compared the performance against an OFDM system that does not use multiple description coding. Results indicate improvement can be achieved by constructing multiple independent bitstreams using UEP techniques.

Appendix

A. Packet Loss PMF of a Single Channel

In [33], Zorzi *et al.* show that at the block/packet level, the binary process which describes the success or failure of packet transmissions in a fading channel can be well-modeled by a two-state Markov chain for a broad range of parameters. A two-state Markov model, which corresponds to a Gilbert–Elliot channel, characterizes the channel by a "good" (G) state and a "bad" (B) state. Let S denote the event that a packet is correctly received, and F denote the event that an erroneous packet is received. In the good state, packets are *always* successfully received

$$P(S|G) = 1, \quad P(F|G) = 0 \tag{8}$$

while in the bad state, packets are *always* corrupted

$$P(S|B) = 0, \quad P(F|B) = 1. \tag{9}$$

To explain the convexity shown in Fig. 7, instead of assuming $P(S|G) = 1$ and $P(S|B) = 0$ in the classical 2-state model, we consider a more general 2-state model

$$P(S|G) = 1 - \epsilon_1, \quad P(F|G) = \epsilon_1 \tag{10}$$

$$P(S|B) = \epsilon_2, \quad P(F|B) = 1 - \epsilon_2 \tag{11}$$

for some small finite positive numbers ϵ_1 and ϵ_2. Notice that when both ϵ_1 and ϵ_2 are zero, the modified model is the same as the classical model. Let $P_{\mathcal{M}}(m)$ denote the probability that m packets are corrupted for a channel with M correlated subcarriers. Based on the modified model, we shall show that $P_{\mathcal{M}}(m)$ is convex if and only if $\epsilon_1, \epsilon_2 \leq 1/(M+1)$.

Using Bayes' rule, we have

$$P_{\mathcal{M}}(m) = P_{\mathcal{M}}(m|G)P(G) + P_{\mathcal{M}}(m|B)P(B) \tag{12}$$

where

$$P_{\mathcal{M}}(m|G) = \binom{M}{m} \epsilon_1^m (1-\epsilon_1)^{M-m} \tag{13}$$

and

$$P_{\mathcal{M}}(m|B) = \binom{M}{m} (1-\epsilon_2)^m \epsilon_2^{M-m}. \tag{14}$$

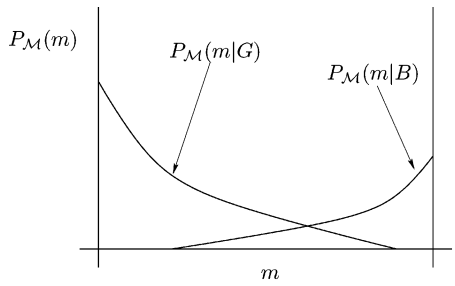

Fig. 16. Packet loss PMF plot for a nonselective fading channel consisting of M correlated subcarriers.

Since $P_{\mathcal{M}}(m|G)$ and $P_{\mathcal{M}}(m|B)$ are binomially distributed, we must have both $P_{\mathcal{M}}(m|G)$ and $P_{\mathcal{M}}(m|B)$ monotonic, as illustrated in Fig. 16.

Consider the ratio

$$\frac{P_{\mathcal{M}}(m|G)}{P_{\mathcal{M}}(m+1|G)} = \frac{\binom{M}{m} \epsilon_1^m (1-\epsilon_1)^{M-m}}{\binom{M}{m+1} \epsilon_1^{m+1} (1-\epsilon_1)^{M-m-1}} = \frac{m+1}{M-m} \cdot \frac{1-\epsilon_1}{\epsilon_1}. \tag{15}$$

For $P_{\mathcal{M}}(m|G)$ to be strictly decreasing with m

$$\frac{m+1}{M-m} \cdot \frac{1-\epsilon_1}{\epsilon_1} \geq 1, \qquad \forall m \in [0, M]$$

$$\Leftrightarrow \quad \epsilon_1 \leq \frac{m+1}{M+1}$$

$$\Leftrightarrow \quad \epsilon_1 \leq \frac{1}{M+1}. \tag{16}$$

Similarly, by considering the monotonically increasing property of $P_{\mathcal{M}}(m|B)$, we have

$$\epsilon_2 \leq \frac{1}{M+1}. \tag{17}$$

Hence, $P_{\mathcal{M}}(m)$ is convex with a global minimum as shown if and only if $\epsilon_1, \epsilon_2 \leq 1/(1+M)$.

B. Packet Loss PMF for N Independent Channels

In this section, we provide a brief explanation for the simulation results presented in Fig. 8. In the figure, we show the joint PMF of the number of packet losses, $P_{\mathcal{J}}(j)$, for N independent channels, each consisting of M correlated subcarriers. When N is small, $P_{\mathcal{J}}(j)$ exhibits local maxima at integral multiples of M, and the variance of $P_{\mathcal{J}}(j)$ decreases as N increases.

Let $P_{\mathcal{M}}(m_i)$ be the PMF of the packet losses of channel i, where $M_i \in [0, M], \forall i$. The joint PMF $P_{\mathcal{J}}(j)$ can be obtained by standard approaches using the characteristic function for $P_{\mathcal{M}}(m)$, or through convolution [42]. Alternatively, the joint PMF can be found by exhausting all possibilities that the sum of N positive integers can equal value j. Hence, we have

$$P_{\mathcal{J}}(j) = \sum_{\{m_1,\ldots,m_N : j = m_1 + \cdots + m_N\}} P_{\mathcal{M}}(m_1) \cdots P_{\mathcal{M}}(m_N). \tag{18}$$

Therefore, $P_{\mathcal{J}}(j)$ is determined by the number of combinations for j and $P_{\mathcal{M}}(m_i)$. As $n \to \infty$, by the Central Limit Theorem, $P_{\mathcal{J}}(j)$ approaches a normal distribution, as illustrated

in Fig. 8. However, for small N, due to the limited number of combinations for j, $P_{\mathcal{J}}(j)$ is predominately determined by the PMFs $(P_{\mathcal{M}}(m))$ of the individual channels. Since $P_{\mathcal{M}}(m)$ exhibits local maxima at $m = 0$ and $m = M$, $P_{\mathcal{J}}(j)$ shows local maxima at integral multiples of M for small N, as illustrated in Fig. 8.

REFERENCES

[1] L. Zheng and D. N. C. Tse, "Diversity and multiplexing: A fundamental tradeoff in multiple-antenna channels," *IEEE Trans. Inf. Theory*, vol. 49, no. 5, pp. 1073–1096, May 2003.

[2] J. N. Laneman, E. Martinian, G. W. Wornell, J. G. Apostolopoulos, and S. J. Wee, "Comparing application- and physical-layer approaches to diversity on wireless channels," in *Proc. ICC*, vol. 4, Anchorage, AK, May 2003, pp. 2678–2682.

[3] X. Yang and K. Ramchandran, "Optimal subband filter banks for multiple description coding," *IEEE Trans. Inf. Theory*, vol. 46, no. 7, pp. 2477–2490, Nov. 2000.

[4] L. Ozarow, "On a source-coding problem with two channels and three receivers," *Bell Syst. Tech. J.*, vol. 59, pp. 1909–1921, 1980.

[5] A. El Gamal and T. M. Cover, "Achievable rates for multiple descriptions," *IEEE Trans. Inf. Theory*, vol. IT-28, no. 5, pp. 851–857, Nov. 1982.

[6] J. K. Wolf, A. D. Wyner, and J. Ziv, "Source coding for multiple descriptions," *Bell Syst. Tech. J.*, vol. 59, no. 8, pp. 1417–1426, Oct. 1980.

[7] V. K. Goyal, "Multiple description coding: Compression meets the network," *IEEE Signal Process. Mag.*, no. 9, pp. 74–93, Sep. 2001.

[8] V. Vaishampayan, "Design of multiple description scalar quantizers," *IEEE Trans. Inf. Theory*, no. 3, pp. 821–834, May 1993.

[9] Y. Wang, M. T. Orchard, V. Vaishampayan, and A. R. Reibman, "Multiple description coding using pairwise correlating transforms," *IEEE Trans. Image Process.*, vol. 10, no. 5, pp. 351–366, May 2001.

[10] J. K. Rogers and P. C. Cosman, "Wavelet zerotree image compression with packetization," *IEEE Signal Process. Lett.*, vol. 5, no. 5, pp. 105–107, May 1998.

[11] A. E. Mohr, E. A. Riskin, and R. E. Ladner, "Graceful degradation over packet erasure channels through forward error correction," *Proc. IEEE Data Compression Conf.*, pp. 92–101, Mar. 1999.

[12] R. Puri, S. S. Pradhan, and K. Ramchandran, "n-channel symmetric multiple descriptions—Part II: (n, k) source channel erasure codes," *IEEE Trans. Inf. Theory*, to be published.

[13] J. Apostolopoulos, W.-T. Tan, S. Wee, and G. W. Wornell, "Modeling path diversity for multiple description video communication," *Proc. IEEE ICASSP*, vol. 3, pp. 13–17, May 2002.

[14] J. G. Apostolopoulos, "Reliable video communication over lossy packet networks using multiple state encoding and path diversity," *Proc. SPIE*, pp. 392–409, Jan. 2001.

[15] W. Xu and L. B. Milstein, "On the performance of multicarrier RAKE systems," *IEEE Trans. Commun.*, vol. 49, no. 10, pp. 1812–1823, Oct. 2001.

[16] D. G. Sachs, R. Anand, and K. Ramchandran, "Wireless image transmission using multiple-description based concatenated codes," *Proc. SPIE*, vol. 3974, pp. 300–311, Jan. 2000.

[17] Y. Sun, Z. Xiong, and X. Wang, "Scalable image transmission over differentially space-time coded OFDM systems," *Proc. GlobeCom*, vol. 1, pp. 379–383, Nov. 2002.

[18] A. Albanese, J. Blomer, J. Edmonds, M. Luby, and M. Sudan, "Priority encoded transmission," *IEEE Trans. Inf. Theory*, vol. 46, no. 6, pp. 1737–1744, Nov. 1996.

[19] R. Puri and K. Ramchandran, "Multiple description source coding using forward error correction codes," in *Proc. 33rd Asilomar Conf. Signals, Systems and Computer*, Pacific Grove, CA, Oct. 1999, pp. 342–346.

[20] A. Said and W. A. Pearlman, "A new, fast, and efficient image codec based on set partitioning in hierarchical trees," *IEEE Trans. Circuits Syst. Video Technol.*, vol. 6, no. 6, pp. 243–249, Jun. 1996.

[21] K.-P. Ho and J. M. Kahn, "Transmission of analog signals using multicarrier modulation: A combined source-channel coding approach," *IEEE Trans. Commun.*, vol. 44, no. 11, pp. 1432–1443, Nov. 1996.

[22] J. M. Cioffi. *Lecture Notes for EE379C Advanced Digital Communication* [Online]. Available: http://www.stanford.edu/class/ee379c/

[23] J. Song and K. J. R. Liu, "Robust progressive image transmission over OFDM systems using space-time block code," *IEEE Trans. Multimedia*, vol. 4, no. 3, pp. 394–406, Sep. 2002.

[24] C.-H. Kuo, C.-S. Kim, and C.-C. J. Kuo, "Robust video transmission over wideband wireless channel using space-time coded OFDM systems," in *Proc. IEEE WCNC*, vol. 2, Mar. 2002, pp. 931–936.

[25] J. Xu, Q. Zhang, W. Zhu, X.-G. Xia, and Y.-Q. Zhang, "Optimal joint source-channel bit allocation for MPEG-4 fine granularity scalable video over OFDM system," in *IEEE Proc. ISCAS*, vol. 2, Bangkok, Thailand, May 2003, pp. 360–363.

[26] P. J. Cherriman, T. Keller, and L. Hanzo, "Subband-adaptive turbo-coded OFDM-based interactive video telephony," *IEEE Trans. Circuits, Syst., Video Technol.*, vol. 12, no. 10, pp. 829–839, Oct. 2002.

[27] R. Puri, K.-W. Lee, K. Ramchandran, and V. Bharghavan, "An integrated source transcoding and congestion control paradigm for video streaming in the internet," *IEEE Trans. Multimedia*, vol. 3, no. 1, pp. 18–32, Mar. 2001.

[28] S. S. Pradhan, R. Puri, and K. Ramchandran, "n-channel symmetric multiple descriptions - part I: (n, k) source channel erasure codes," *IEEE Trans. Inf. Theory*, vol. 50, no. 1, pp. 47–61, Jan. 2004.

[29] R. J. McEliece and W. E. Stark, "Channels with block interference," *IEEE Trans. Inf. Theory*, vol. IT-30, no. 1, pp. 44–53, Jan. 1984.

[30] M. Medard and R. G. Gallager, "Bandwidth scaling for fading multipath channels," *IEEE Trans. Inf. Theory*, vol. 48, no. 4, pp. 840–852, Apr. 2002.

[31] E. Malkamaki and H. Leib, "Performance of truncated type-II hybrid ARQ schemes with noisy feedback over block fading channels," *IEEE Trans. Commun.*, vol. 48, no. 9, pp. 1477–1487, Sep. 2000.

[32] R. Knopp and P. A. Humblet, "On coding for block fading channels," *IEEE Trans. Inf. Theory*, vol. 46, pp. 189–205, Jan. 2000.

[33] M. Zorzi, R. R. Rao, and L. B. Milstein, "Error statistics in data transmission over fading channels," *IEEE Trans. Commun.*, vol. 46, no. 11, pp. 1468–1477, Nov. 1998.

[34] H. Bischl and E. Lutz, "Packet error rate in the noninterleaved Rayleigh channel," *IEEE Trans. Commun.*, vol. 43, no. 2–4, pp. 1375–1382, Feb./Mar./Apr. 1995.

[35] V. M. Stankovic, R. Hamzaoui, and Z. Xiong, "Real-time error protection of embedded codes for packet erasure and fading channels," *IEEE Trans. Circuits, Syst., Video Technol.*, vol. 14, no. 8, pp. 1064–1072, Aug. 2004.

[36] S. Dumitrescu, X. Wu, and Z. Wang, "Globally optimal uneven error-protected packetization of scalable code streams," *IEEE Trans. Multimedia*, vol. 6, no. 2, pp. 230–239, Apr. 2004.

[37] T. Stockhammer and C. Buchner, "Progressive texture video streaming for lossy packet network," presented at the 11th Packet Video Workshop, Kyongju, Korea, May 2001.

[38] A. E. Mohr, R. E. Ladner, and E. A. Riskin, "Approximately optimal assignment for unequal loss protection," in *Proc. Int. Conf. Image Processing*, vol. 1, Sep. 2000, pp. 367–370.

[39] J. G. Proakis, *Digital Communications*, 2nd ed. New York: McGraw-Hill, 1989.

[40] Y. R. Zheng and C. Xiao, "Simulation models with correct statistical properties for Rayleigh fading channels," *IEEE Trans. Commun.*, vol. 51, no. 6, pp. 920–928, Jun. 2003.

[41] V. Chande and N. Farvardin, "Progressive transmission of images over memoryless noisy channels," *IEEE J. Sel. Areas Commun.*, vol. 18, no. 6, pp. 850–860, Jun. 2000.

[42] A. Papoulis and S. U. Pilla, *Probability, Random Variables and Stochastic Processes*, 4th ed. New York: McGraw-Hill, 2001.

Yee Sin Chan (S'00–M'03) received the B.Eng. (Hon.) degree in electrical and electronic engineering from the University of Hong Kong (HKU), the M.Phil. degree in physics from the Hong Kong University of Science and Technology (HKUST), and the M.Sc. and Ph.D. degrees in electrical engineering from Rensselaer Polytechnic Institute (RPI), Troy, NY.

He is currently a Postdoctoral Research Scientist at the University of California at San Diego, La Jolla. His research interests lie in the areas of communications, signal processing, and information theory.

Dr. Chan is a member of Sigma Xi. He is the recipient of several awards, including the Sir Edward Youde Fellowship from the Hong Kong Government, the Y. L. Liu Fellowship from RPI, and the Joyce M. Kuok Scholarship from HKU.

Pamela C. Cosman (S'88–M'93–SM'00) received the B.S. degree (with honors) in electrical engineering from the California Institute of Technology, Pasadena, in 1987, and the M.S. and Ph.D. degrees in electrical engineering from Stanford University, Stanford, CA, in 1989 and 1993, respectively.

She was an NSF Postdoctoral Fellow at Stanford University and a Visiting Professor at the University of Minnesota, Minneapolis, from 1993 to 1995. Since July 1995, she has been with the faculty of the Department of Electrical and Computer Engineering, University of California at San Diego, La Jolla, where she is currently a Professor and Co-Director of the Center for Wireless Communications. Her research interests are in the areas of image and video compression and processing.

Dr. Cosman is a member of Tau Beta Pi and Sigma Xi. She is the recipient of the ECE Departmental Graduate Teaching Award (1996), a Career Award from the National Science Foundation (1996 to 1999), and a Powell Faculty Fellowship (1997 to 1998). She was an Associate Editor of the IEEE COMMUNICATIONS LETTERS (1998 to 2001), a Guest Editor of the June 2000 special issue of the IEEE JOURNAL ON SELECTED AREAS IN COMMUNICATIONS on "error-resilient image and video coding," and the Technical Program Chair of the 1998 Information Theory Workshop, San Diego. She was an Associate Editor of the IEEE SIGNAL PROCESSING LETTERS (2002 to 2005). She was a Senior Editor (2003 to 2005) and is currently the Editor-in-Chief of the IEEE JOURNAL ON SELECTED AREAS IN COMMUNICATIONS. Her Web page address is http://www.code.ucsd.edu/cosman/.

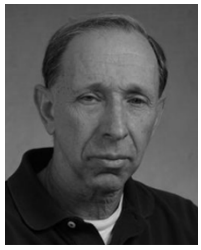

Laurence B. Milstein (S'66–M'68–SM'75–F'85) received the B.E.E. degree from the City College of New York, New York, in 1964, and the M.S. and Ph.D. degrees in electrical engineering from the Polytechnic Institute of Brooklyn, Brooklyn, NY, in 1966 and 1968, respectively.

From 1968 to 1974, he was with the Space and Communication Group of Hughes Aircraft Company, and from 1974 to 1976, he was a Member of the Department of Electrical and Systems Engineering, Rensselaer Polytechnic Institute, Troy, NY. Since 1976, he has been with the Department of Electrical and Computer Engineering, University of California at San Diego (UCSD), La Jolla, where he is a Professor and former Department Chairman, working in the area of digital communication theory, with special emphasis on spread-spectrum communication systems. He has also been a Consultant to both government and industry in the areas of radar and communications.

Dr. Milstein was an Associate Editor for Communications Theory for the IEEE TRANSACTIONS ON COMMUNICATIONS, an Associate Editor for Book Reviews for the IEEE TRANSACTIONS ON INFORMATION THEORY, an Associate Technical Editor for the IEEE COMMUNICATIONS MAGAZINE, and the Editor-in-Chief of the IEEE JOURNAL ON SELECTED AREA IN COMMUNICATIONS. He was the Vice President for Technical Affairs in 1990 and 1991 of the IEEE Communications Society, and has been a member of the Board of Governors of both the IEEE Communications Society and the IEEE Information Theory Society. He is a former Chair of the IEEE Fellows Selection Committee and a former Chair of ComSoc's Strategic Planning Committee. He is a recipient of the 1998 Military Communications Conference Long-Term Technical Achievement Award, an Academic Senate 1999 UCSD Distinguished Teaching Award, an IEEE Third Millennium Medal in 2000, the 2000 IEEE Communications Society Armstrong Technical Achievement Award, and the 2002 MILCOM Fred Ellersick Award.